Reduction of the Uncertainties in the Hydrological Projections in Korean River Basins Using Dynamically Downscaled Climate Projections

Liying Qiu
The Hong Kong University of Science and Technology

Joeng-Bae Kim
Sejong University

Seon-Ho Kim
Sejong University

Yeon-Woo Choi
Massachusetts Institute of Technology

Eun-Soon Im (✉ ceim@ust.hk)
The Hong Kong University of Science and Technology   https://orcid.org/0000-0002-8953-7538

Deg-Hyo Bae
Sejong University

Research Article

1 **Reduction of the uncertainties in the hydrological projections in Korean**
2 **river basins using dynamically downscaled climate projections**

3

4 **Liying Qiu[1+], Joeng-Bae Kim[2+], Seon-Ho Kim[2], Yeon-Woo Choi[3], Eun-Soon Im[*1,4] and Deg-**
5 **Hyo Bae[2]**

6

7 [1]Department of Civil and Environmental Engineering, The Hong Kong University of Science and Technology,
8 Hong Kong SAR, China

9 [2]Department of Civil and Environmental Engineering, Sejong University, Seoul, Korea

10 [3]Ralph M. Parsons Laboratory, Massachusetts Institute of Technology, Cambridge, MA, USA

11 [4]Division of Environment and Sustainability, The Hong Kong University of Science and Technology, Hong
12 Kong SAR, China

13 [+]These authors contributed equally to this work

14

15

16 ***Correspondence to: <u>ceim@ust.hk</u>**

17 **[Corresponding authors]**

18 Prof. Eun-Soon Im

19 E-mail: ceim@ust.hk

20 Address: Academic Building 3594, The Hong Kong University of Science and Technology, Clear Water Bay,
21 Kowloon, Hong Kong, China.

22

23 **ORCID**

24 Liying Qiu (0000-0001-9944-4311)

25 Jeong-Bae Kim (0000-0002-6121-7751)

26 Seon-Ho Kim (0000-0002-1217-2075)

27 Yeon-Woo Choi (0000-0002-3400-6705)

28 Eun-Soon Im (0000-0002-8953-7538)

29 Deg-Hyo Bae (0000-0002-0429-1154)

Abstract

How the added value of dynamically downscaled climate variables can be transferable to the hydrological impact assessment has been a long standing issue. This study investigates the potential benefit of high-resolution climate data locally tailored over South Korea in terms of the reduction of uncertainties in hydrological projections. For this purpose, a large ensemble consisting of three Global Climate Model (GCM) projections and their downscaling products with different resolutions (i.e., 20 and 5 km), and four bias correction (BC) methods is fed into a semi-distributed hydrological model (HM) customized over Korean river basins. The in-depth comparison among the 45-members hydrological simulations proves that the added value of RCM would not be erased by the application of BC. While this study acknowledges the necessity of BC to remove the systematic bias in climate simulations, it is found that the high-resolution dynamical downscaling can significantly narrow the spread brought with different BC methods, thus reducing the uncertainty in the projected hydrological change. The projected streamflow changes for both the mean of wet season and the high flows indicate that there will be an intensified runoff, especially for the extremes, over South Korea under the warming. Altogether, this study provides a valuable exploration of uncertainty reduction in hydrological projections from the perspective of resolution effect of dynamical downscaling, which is meaningful for hydroclimate studies and climate change impact assessment.

Keywords

Uncertainty in hydrological projections, dynamical downscaling, bias correction, Korean river basin

Declarations

Funding

Conflicts of interest

The authors declare that the research was conducted in the absence of any commercial or financial relationships that could be construed as a potential conflict of interest.

Availability of data and material

The CMIP5 data is available from ESGF repository (https://esgf-node.llnl.gov/projects/cmip5/). Other data that support the findings of this study are available from the corresponding author upon reasonable request.

Code availability

The authors used R packages "downscaleR" (version 3.1.0) and "MBC" (version 0.10-5) for BC, and VIC hydrological model for shydrological simulation, which are all free online.

1 Introduction

One of the most critical impacts of climate change that needs deep understanding and profound planning is the change in the Earth's hydrological cycle. It is expected that the river flows will witness substantial transitions affected by the changes in multiple processes under the global warming. For example, the exposure to flood hazards will continue to increase as the heavy rainfall increases under global warming on a local scale (Kundzewicz et al. 2014). Almost all of the physical processes included in the hydrological cycle, e.g., precipitation, evapotranspiration, infiltration, runoff, and routing, will be affected by the increasing temperature and relevant water vapor change, either directly or indirectly (Held and Soden 2006). Such changes in the water cycle should be carefully studied because they may impact the entire environment or even cause severe disasters. The reliable hydrological projections under global warming are thus urgently needed for the timely planning of water resource management and mitigation of the possible damages (Sun et al. 2017).

Currently, the hydrological projections are usually realized in a modeling chain consisting of climate models (CMs), bias corrections (BCs), and hydrological model (HMs) (Teutschbein and Seibert 2012; Muerth et al. 2013), which covers the numerical simulations of various physical processes and the statistical correction based on observed meteorological conditions. In this case, although HM is the last and direct tool for the streamflow simulation, the quality of hydrological projections is yet highly dependent on the reliability of the meteorological input into the HMs. The uncertainty sources of hydrological projections have been quantified in the previous studies for different regions around the world. These studies generally reach a similar conclusion that for most regions, CMs act as the leading source of uncertainty for the wet season or high flow projections (e.g., Aryal et al. 2019; Zhang et al. 2021), whereas HMs may contribute more to the uncertainty of dry season or low flow projections (e.g., Vetter et al. 2017; Lee et al. 2021). Also, the interactions among the uncertainty factors are non-negligible and may even play a larger role than the individual sources (Bosshard et al. 2013; Vetter et al. 2015; Zhang et al. 2021). For example, the impact of BC on runoff will increase with the bias of CMs (Muerth et al. 2013), because the correcting coefficient is scaled by the deviation of historical climate simulations from the observation. More importantly, considering the complicated and non-linear processes evolved in the climate system, the assumption of stationary bias for the present and future climate simulations used by BC (Teutschbein and Seibert 2012) is likely to distort the projected relative change if the correcting factor is too large.

To improve the reliability of meteorological input to the hydrological projections, one of the most popular approaches is to downscale the coarse-resolution climate simulations from the Global Climate Models (GCMs) by the Regional Climate Models (RCMs). Since the surface hydrological processes typically occur on scales finer than GCMs, RCMs can help to reduce the resolution gap and improve the quality of modeled meteorological conditions by resolving the small-scale processes. During the past decade, there have already been considerable efforts to apply and evaluate the benefits of dynamical downscaling products in hydrological impact assessments (Kotamarthi et al. 2021). However, the current typical grid size of 10-50 km (e.g., Giorgi and Gutowski 2015; Jacob et al. 2020) employed in RCMs still cannot meet the desirable spatial scale and information quality required by HMs. For example, the bias in the estimation of rainfall-driven flood can be largely attributed to the underestimation of daily precipitation variability and extreme events in the climate simulations. To resolve such problems and reduce the subsequent uncertainty in hydrological projections, the most straightforward and reliable way is to increase the resolution of RCMs (Qiu et al. 2020), which can enhance the reliability of the regional climate projections through a better representation of the complex topography and physical mechanisms.

On the other hand, although there is a growing consensus regarding the necessity of reliable meteorological

112   input for HMs (Maraun et al. 2010), there are few explicit assessments of how the high-resolution RCMs
113   help to reduce the uncertainty in hydrological projections. Especially under the extensive use of BC
114   techniques, many studies are not aware of, or not clear about, how the quality of original climate simulations
115   affects the reliability of hydrological impact assessments. Quite a few hydrological projections are still using
116   GCM simulations processed only with simple interpolation and BC (e.g., Stefanidis et al. 2018; Zaman et al.
117   2018; Anjum et al. 2019; Haider et al. 2020), despite the apparent incompatibility in the scale of the CM and
118   HM. Even for those using the RCM products, they might also be uncertain about how dynamical downscaling
119   and BC are affecting the results (Maraun et al. 2010). As a post-processing tool for climate model output, BC
120   is useful but the application without good understanding of its relationship with the climate simulation may
121   lead to problematic conclusions. It is warned that BC may have limited ability to correct and downscale
122   variability, and it may even provide implausible climate change signals (Maraun et al. 2017). Thus, an
123   integrated assessment should be made regarding how dynamical downscaling aids in the uncertainty
124   reduction hydrological projection modeling chain, which is especially meaningful in this era of continuous
125   marching into high-resolution climate simulation.

126   In this study, we conduct a large ensemble of hydrological projections driven by long-term climate change
127   simulations over South Korea from three different resolutions, i.e., three GCMs and their dynamical
128   downscaling products in 20 and 5 km. As a follow-up study of Qiu and Im (2021)[1], this study aims to evaluate
129   and explore how the demonstrated advantage of very-high-resolution (i.e., 5 km) climate simulation benefits
130   the hydrological studies. In this regard, we use four BC methods to process the climate projections of the
131   three resolutions and feed the original and bias-corrected climate data into a designated HM for streamflow
132   projections. Although previous studies have quantified the uncertainty contribution from CM, BC, and HM,
133   we focus on how the combination of very-high-resolution RCM simulations and different BC methods affect
134   the hydrological projection output. The 5-km dynamical downscaling is not only the finest resolution long-
135   term climate projections over this region so far, but more importantly, there have been few hydrological
136   projections driven by RCM products at such a high resolution before despite the study area. Although the
137   very-high-resolution dynamical downscaling has shown an added value over the coarse resolution
138   highlighted by the improved reliability in the projected climate change features, this may seem "useless" to
139   the end-users if no improvements can be seen in the hydrological projections that are run with bias-corrected
140   climate data. Therefore, we adopt BC methods with different levels of complexity to provide a comprehensive
141   comparative assessment for hydrological projections driven by the climate scenarios in different
142   combinations of CM resolution and BC technique. It serves to provide straightforward information for the
143   hydrological modeling community regarding the practical value of the high-resolution dynamical
144   downscaling and the large ensemble of hydrological projections also adds valuable insight into the
145   understanding of the regional water cycle change.

146   **2 Methodology and data**

147   **2.1 Experimental procedure and study area**

148   Fig. 1a presents the experimental framework of this study in three steps: climate simulation, statistical BC,
149   and hydrological simulation with HM. Three Coupled Model Intercomparison Project Phase 5 (CMIP5,
150   Taylor et al 2012) GCM projections under the RCP8.5 scenario and their downscaling products in 20 km and
151   5 km are combined with different BC methods to constitute a 3 [CMIP5 models] × 3 [resolutions] × (4+1)
152   [BC methods] = 45-members ensemble of climate scenarios for driving hydrological simulations. The climate
153   and hydrological simulations both cover 30-yr periods for the reference (REF, 1976-2005) and the future

---

[1] Qiu L, Im E-S (2021) Added value of high resolution climate projections over South Korea on the scaling of precipitation with
temperature. Environ Res Lett. *Under Review*

4

154 (FUT, 2071-2100) over South Korea (Fig. 1b). The Korean Peninsula is a typical region needing high-
155 resolution climate modeling since its hydroclimate characteristics are strongly influenced by the varying
156 geographic features with sharp topographical gradients encompassed by long coastlines. Also, it has been
157 demonstrated the river flows of South Korea will witness substantial changes (Ryu et al. 2011; Jung et al.
158 2013; Seo et al. 2016; Ahn and Kim 2016; Lee et al. 2018a, 2021; Kim et al. 2020) given the condition that
159 the regional climate has been projected to experience a non-trivial change in the future (Seo et al. 2013; Kim
160 et al. 2018; Oh and Suh 2018). Though the simulations covering the whole country, we target over the Han
161 River basin (HRB) and Nakdong River basin (NRB) for the streamflow analyses, which are the two largest
162 river basins in South Korea taking up more than two-thirds of the area and a large portion of the population
163 (Lee et al. 2019b). Meanwhile, to highlight the effect on uncertainty reduction from the climate scenarios,
164 we mostly focus on the performance during the wet season (June to September, JJAS) and the high flows.

165 **2.2 Climate simulations**

166 Table 1 lists the 3 [CMIP5 models] × 3 [resolutions] =9 climate projections under RCP8.5 scenario used in
167 this study. The three CMIP5 models (i.e., CCSM4, NorESM1-M, and HadGEM2-ES, hereinafter as CCSM4,
168 NorESM, and HadGEM2) were carefully selected to cover varying climate sensitivities and they all
169 demonstrated reliable performances over East Asia. Then, a designated one-way double-nested system in the
170 Weather Research and Forecasting model (WRF version 4.2, Skamarock et al. 2019) is used to downscale
171 the three CMIP5 GCM projections into 20 km (hereinafter as WRF20) and 5 km (hereinafter as WRF05).
172 Thus, for each CMIP5 model, we have climate simulations in the three resolutions (i.e., the original GCM,
173 WRF20, and WRF05). The overall performance of the downscaling climate simulations and the added value
174 of WRF05 were comprehensively evaluated in the previous studies (Qiu et al. 2020; Qiu and Im 2021).

175 For driving the hydrological simulations, the daily time series of maximum temperature (Tmax), minimum
176 temperature (Tmin), precipitation, and mean horizontal wind speed of the 9 climate simulations are needed.
177 To resolve the discrepancy among horizontal resolution in the climate simulations, the four meteorological
178 variables are first interpolated by distance-weighted average remapping onto the 0.125° grid (i.e., the grid of
179 VIC simulation) before further post-processing.

180 **2.3 BC methods**

181 The principle of BC is to use observation as predictands for calibrating the simulated predictors. It can be
182 used to correct the systematic bias in CM output, such as the overestimation of the occurrence of wet days
183 and/or the underestimation of heavy precipitation (Maraun 2016). It is used to post-process either GCM or
184 RCM data in almost all hydrological studies. Here, four BC methods are applied to three meteorological
185 variables, i.e., daily Tmax, daily Tmin, and daily precipitation, for evaluating the effect of different
186 combinations of climate simulations and BC methods on hydrological projections. The horizontal wind speed
187 is not corrected because the BC of wind speed has little effect on the runoff projections (Haddeland et al.
188 2012). Instead, for both the hydrological simulation in REF and FUT, the same original wind speed data from
189 REF simulations is used so that no consideration is given to its bias and the change under global warming.

190 The in-situ meteorological data used for correction is from 57 observation stations maintained by the Korean
191 Meteorological Administration (KMA) during 1986-2005 (hereinafter as OBS). The station data is first
192 interpolated onto the 0.125° grid (i.e., the grid of VIC simulation) for consistency with the model data, and
193 then the BC is applied on a grid-point base. A sliding window of three months central with each calendar
194 month is used to consider the seasonality following Teutschbein and Seibert (2012) and Cannon (2018).

195 The four state-of-the-art BC methods used are namely Variance Scaling for temperature and Power
196 Transformation for precipitation (VAPT), Empirical Quantile Mapping (EQM), Quantile Delta Mapping

197 (QDM), and Multivariate Bias Correction with the N-dimensional probability density function (MBCn).
198 Specifically, VAPT, EQM, and QDM are applied by the R package "downscaleR" (version 3.1.0) (Bedia et
199 al. 2020) and MBCn is applied by the R package "MBC" (version 0.10-5) (Cannon 2020). For the comparison,
200 the raw climate simulation output without BC (hereinafter as RAW) is also used for hydrological simulation.
201 Here, we include a brief introduction of the four BC methods below, but more detailed information can be
202 reached from the relevant references.

203 VAPT is the combination of two relatively simple approaches for correcting temperature and precipitation,
204 respectively, based on the monthly mean and variance (Chen and Dudhia 2001; Leander and Buishand 2007).
205 Quantile Mapping (QM) methods are the most popular BC technique and they follow the basic principle to
206 make the Cumulative Distribution Function (CDF) of the modeled data equal to that of the observation after
207 correction. EQM is one of the most extensively used QM methods and it uses the empirical CDF for the
208 correction instead of assuming a parametric distribution (Teutschbein and Seibert 2012). QDM is a more
209 advanced QM method because it tries to preserve the projected relative change in quantiles by removing and
210 adding the future trend before and after QM (Cannon et al. 2015). Lastly, MBCn is a relatively "high-level"
211 approach that uses an image processing technique to conduct multivariate-based BC. Unlike the other three
212 methods that can correct only a single meteorological variable, it is applied to multiple variables at the same
213 time by considering their joint dependence while also preserving the relative change pattern. Fig. 2 shows an
214 illustrative example of the pairwise bivariate correlations for the observation and model output in this study.
215 The correlation pattern in REF corrected by MBCn is more scattered, showing a higher similarity to OBS.
216 The characteristics that the bias-corrected joint dependence in FUT depends on both the MBCn correcting
217 algorithm calibrated for REF and the projected changes in the RAW may make MBCn better than the other
218 three BC methods (Cannon 2018).

2.4 Hydrological simulation

220 To simulate the streamflow over South Korea, the bias-corrected and the RAW meteorological variables are
221 fed into the Variable Infiltration Capacity (VIC) Macroscale Hydrologic Model (Liang et al. 1994; Hamman
222 et al. 2018)) to generate the runoff. For simplicity, the corresponding experiments are called the
223 "Model$_{Resolution-Period\_BC\ method}$". For example, CCSM4$_{WRF20-REF\_VAPT}$ is the 20-km WRF downscaling of CCSM4
224 for the REF period corrected by the VAPT method. Note that "ENS" stands for the ensemble mean of the
225 output from the hydrological simulations driven by CCSM4, NorESM, and HadGEM2 (or ensemble mean
226 of the hydrological output driven by their downscaling products), instead of using the ensemble-mean
227 meteorological inputs to drive the hydrological simulations. And "ENSBC" is used at the subscript for
228 representing the ensemble mean of the hydrological simulations driven by the same CM data but corrected
229 by four different BC methods.

230 VIC is a large-scale, semi-distributed HM that has been applied widely for the analysis and assessments of
231 climate change impacts on water resources by being coupled to different climate scenarios (e.g., Liang et al.
232 1994; Bae et al. 2015). A 0.125° grid system covering South Korea except for the Jeju Island represented as
233 575 grid points is employed by VIC in this study (Fig. 1b). For hydrological simulations in the VIC, the
234 geophysical datasets with the different spatial resolutions are collected from various sources and aggregated
235 onto the 0.125° grid. The 100-m Digital elevation model (DEM) data is obtained from the Korean National
236 Geographic Information Institute (NGII Korea). Soil data with a 1: 25,000 scale map is from Korea Rural
237 Development Administration (RDA), and land cover data with a 1-km resolution is collected from the Water
238 Resources Management Information System (WAMIS) of Korea. The VIC physics configuration follows
239 Kim et al. (2020) that is set up specifically for this region and it has been proved to show optimal performance
240 through sensitivity tests. Here, we perform an observational run for the validation of HM performance, in
241 which precipitation observation during 1986-2005 maintained by the Korea Ministry of Environment (MOE)

242   from WAMIS is additionally used for the forcing together with the KMA OBS data mentioned in Section 2.3.
243   Fig. 3 shows the daily time series (left column) during REF of the simulated streamflow from the validation
244   run and the measured streamflow. Since streamflow measurement is only available over specific sites (e.g.,
245   dam), the Chungju and Andong dams are selected respectively for the two target river basins. The in-situ
246   measured daily inflow at the two dams were collected by WAMIS, and the simulation values are obtained by
247   adding all the runoff values of VIC grids within the Chungju and Andong dam basins. Such a validation
248   process has been widely used for the HM without horizontal routing module (Safeeq et al. 2014; Kim et al.
249   2020). The time series shows that the simulated streamflow well follows the measured dam inflows both in
250   terms of the temporal variation and the runoff magnitude. The Nash-Sutcliffe efficiency (NSE) and percent
251   bias (PBIAS) of the VIC model are 0.70/0.71 and -2.3%/-3.55% for Chungju/Andong dam basin respectively.
252   These statistics demonstrate the ability of the VIC to capture the streamflow variability. Apart from the time
253   series, Fig. 3 (right column) also provides a day-to-day validation based on the streamflow intensity. It shows
254   that the HM better captures the high flows than the low flows that it may overestimate the flow less than 10
255   CMS. However, the simulation also tends to underestimate the high flows for the extreme tail, which may be
256   due to the insufficient resolution in the OBS data, which has been smoothed due to the interpolation process,
257   especially for the extremely heavy precipitation cases.

258   **3 Result**

259   **3.1 The effect of multiple BC methods on precipitation and temperature**

260   Before the streamflow projections, we first have a look at the precipitation and temperature in different
261   combinations of climate simulations and BC methods. Fig. 4 presents the spatial pattern of the climatological
262   mean Tmax, Tmin, and precipitation in ENS_{REF} and the OBS in JJAS for reference. It is clear that all the four
263   BC methods tend to reduce the bias in the climate simulations, regardless of how large the bias in the raw
264   output is (e.g., precipitation in $ENS_{GCM-REF\_RAW}$). Although slight differences exist among different BC
265   methods, all of them show similarly good performance in terms of the seasonal mean, which is not surprising
266   because BC methods are usually well designed for calibrating the monthly mean.

267   Then, following Cannon et al. (2015) and Seo et al. (2019), several Expert Team on Climate Change
268   Detection and Indices (ETCCDI) indices (Zhang et al. 2011) are used for evaluating the performance of the
269   BC methods. Seo et al. (2019) suggested that 7 ETCCDI indices together with the annual mean can be used
270   as the representative meteorological indices for regional hydrologic impact studies. Here, we exclude those
271   indices more related with the dry season or low flows and additionally include two precipitation indices.
272   Altogether, 6 ETCCDI indices (Table 2) are calculated from all the 45 climate scenarios on a grid-point base.
273   These indices cover both those for the extremes (e.g., Rx1day) and those for the annual mean/accumulation
274   (e.g., SDII). Also, we include the JJAS mean of precipitation, Tmax, and Tmin instead of the annual mean in
275   the evaluation, thus the 9 indices altogether can give a comprehensive assessment of the BC methods
276   regarding the climate indices for hydrologic impact studies during the wet season.

277   The distributions of the 9 indices during REF from the model are evaluated against those from OBS using
278   Kolmogorov-Smirnov (K-S) test at a 1% significance level. A detailed technical explanation can be found in
279   Cannon et al. (2015). Fig. 5 shows the proportion of grid points passing local K-S diagnostic tests for each
280   index in each climate scenario, with warm colors standing for a higher proportion and thus better performance.
281   The test result indicates a significant bias in the simulated distribution of the indices in RAW climate
282   simulations. With the downscaling of increasing resolution (GCM-WRF20-WRF05), the bias reduces but
283   still exists. BC helps to significantly improve the modeled distribution that the portion of grid points passing
284   K-S exceeds 90% for most indices, except for CWD and SDII, which demonstrates the necessity of BC as a
285   pre-processing tool for hydrological simulations. Also, for TN90p in $NorESM_{GCM-REF}$, it seems that BC
286   cannot improve its annual distribution. Comparatively, despite the resolution of the models, the performance

7

287   of BC methods can be roughly ranked as MBCn > QDM > EQM > VAPT, which generally corresponds with
288   their degree of complexity and the computation cost. On the other hand, although BC can significantly reduce
289   the bias in the RAW, it does not mean that the quality of the RAW climate simulations is not meaningful.
290   Instead, even after BC, WRF05 still overweighs WRF20 in the K-S test, not to mention the original GCM. It
291   indicates that the added value of high-resolution RCM would not be erased under the use of BC. Instead, the
292   hybrid of WRF05 with MBCn, i.e., the best-performing dynamical downscaling with best-performing BC
293   approach, yields a pass-portion of over 90% for all the indices including CWD, SDII, and TN90p for NorESM.
294   While the bias-corrected result of the climatological mean seems to be independent of the quality of the RAW
295   simulation, which is also a common skepticism about the necessity of dynamical downscaling (Lee et al.
296   2018b), this result proves that the quality of RAW still affects the extreme statistics even after BC. It is
297   because that if the deviation of the original model simulation is prominent from the observation, the
298   correction factors will also be large, potentially destructing the distribution of extremes that are often non-
299   linear to the climatological mean.

300   Moving to how the BC affects the projected change in precipitation and temperature, Fig. 6 shows the relative
301   change of the climatological mean in JJAS. Although all the BC methods retain the change signs from the
302   RAW, the discrepancy between the relative change in the bias-corrected products and that in the RAW varies
303   with the CM resolution. It is within only ±3% for WRF05, but that in the GCMs is much larger. Especially,
304   the EQM-corrected changes in Tmax and Tmin for ENS_{GCM} are much higher than the others; and the VAPT-
305   and EQM- corrected changes in precipitation also show more than 9% deviation from RAW in this case. Here,
306   VAPT and EQM, compared to QDM and MBCn, do not give consideration to preserving the change trend
307   during the correction processes. While this will not significantly affect the result of the high-resolution
308   downscaled climate variables, it can lead to a large deviation from the RAW in the coarse resolution run
309   given its large bias in the original climate simulations.

310   For zooming into the difference of projected change of the four BC methods, distributions over South Korea
311   of the projected relative changes in the mean Tmax, Tmin, precipitation, and Rx5day as a representative of
312   extreme precipitation, are displayed in Fig. 7. The black is drawn from the RAW, while the colored boxes are
313   from the bias-corrected distributions. It shows that in the coarse resolution, the spatial variation is relatively
314   smaller than in the high resolution, especially for precipitation and its extreme. BC can increase the spatial
315   variability for all the simulations, but the resulted distributions from different BC methods also show
316   differences. Among the four BC techniques applied, the delta method is adopted in QDM and MBCn that it
317   may help them to preserve the change trend across different quantiles by design. EQM and VAPT, on the
318   other, show large positive outliers compared to the RAW, which is also shown in Cannon et al. (2015). Here,
319   in the ENS_{GCM}, the changes in EQM-corrected mean Tmax and Tmin are larger than those corrected by other
320   methods, and the changes in mean precipitation and Rx5day also show a large spread when corrected with
321   different BC methods. For example, for Rx5day, the median in ENS_{GCM_VAPT} is around 10% higher than
322   ENS_{GCM_MBCn}. Comparatively, such a difference becomes much smaller as the resolution increases with
323   downscaling. In ENS_{WRF05}, the larger change for EQM-corrected temperatures becomes smaller; and more
324   importantly, it shows a primarily similar distribution for the precipitation change corrected by the four BC
325   methods.

326   As a whole, BC shows remarkable performance in reducing the bias of the CM simulations, both for the
327   mean and the extremes. Considering both the REF and FUT periods, QDM and MBCn outweigh VAPT and
328   EQM, while MBCn also shows unique privilege in additionally preserving inter-dependence among the
329   corrected variable. However, the results across different climate simulations corrected by different BC
330   methods prove that the added value of dynamical downscaling, including that of increasing resolution, still
331   exists even after applying BC. The best combination of "CM-BC" evaluated here is "WRF05-MBCn".

3.2 Reducing the uncertainty in historical streamflow simulation

In this section, we turn our focus onto the simulated streamflow for the REF period driven by the modeled meteorological variables, using the OBS-driven VIC simulation as the reference for validation. First, the analysis begins with the climatological monthly total runoff over the two basins (Fig. 8). The shaded area is from the OBS run; the black dashed lines mark the hydrological simulations driven by RAW and the colored lines delegate those driven by the bias-corrected meteorological conditions. Not surprisingly, there is little difference brought by different BC methods on the monthly time scale, which is consistent with the finding in Section 3.1. Also, compared to the RAW, BC improves the simulated runoff for all the models and resolutions. On the other hand, discrepancies among the CMIP5 models and the CM resolutions can be found. All the three original GCMs underestimate the peaks of streamflow in the wet season for the two basins. Although BC helps reduce such biases, the bias is still found especially for $CCSM4_{GCM-REF}$ over HRB and $HadGEM2_{GCM-REF}$ over NRB. The BC procedure that the correcting coefficient is obtained from a 90-day window centered for individual months may explain the bias in the annual cycle. If the bias in the original climate simulation is too large, then the effect of the 90-day window will also be noticeable on the monthly statistics, though it may not be obvious when considering the seasonal mean. Comparatively, the downscaling with WRF improves the simulated annual cycle so that the simulated runoff after BC is much closer to the OBS. Here, the performances of WRF20 and WRF05 with BC are similar, which is reasonable since WRF20 has also been proved to perform well for the climatological monthly statistics in the previous study (Qiu et al. 2020). Fig. 8 also indicates a clear annual phase of the streamflow over South Korea. While the hydrological simulations driven by bias-corrected meteorological conditions can generally capture the entire annual cycle indicated in the OBS run, this study mainly focuses on the "wet season" defined as June to September that is a period with higher runoff.

Fig. 9a presents the mean for the wet season from ENS_{GCM}, ENS_{WRF20}, and ENS_{WRF05} to evaluate the spatial patterns of the simulated runoff. The result shows that more extensive runoff is found for the HRB than the NRB, and the NRB shows higher runoff on the south than the north. Such spatial characteristics are missed in $ENS_{GCM-REF\_RAW}$, accompanied by a significant underestimation in the magnitude. Downscaling much improves the spatial variation while $ENS_{WRF05-REF\_RAW}$ reduces the wet bias in $ENS_{WRF20-REF\_RAW}$. For all the resolutions, BC significantly helps improve the simulated runoff. It reduces the bias in the runoff magnitude and improves the spatial distribution, which results in the highly similar patterns of the wet season mean runoff despite the BC methods used and the original climate simulation resolution.

For the mean of the annual maximum daily streamflow (AMDS), which is one of the indices for representing the high flows (Lee et al. 2019a) (Fig. 9b), $ENS_{GCM-REF\_RAW}$ again barely captures either the magnitude or spatial distribution. The downscaling effectively demonstrates the effect of resolution in improving the reproduction of spatial variability, but it also inherits the problem of overestimation from the precipitation representation (Qiu and Im 2021). However, as mentioned in Section 2.4, it should also be noted that the hydrological simulation driven by interpolated station data (i.e., the OBS run) may have the problem of underestimated high flow, especially for the extremely heavy case. The application of BC, while greatly improving the performance of $ENS_{GCM-REF}$ and also reducing the overestimation in NRB for $ENS_{WRF20-REF}$ and $ENS_{WRF05-REF}$, seems to "over-correct" the high flow for HRB in the hydrological simulations driven by downscaled products. The high flows in HRB from the simulations with BC show a larger discrepancy from OBS than those with RAW. This may be due to the fact that the BC coefficients for precipitation in WRF20 and WRF05 are primarily scaled by the majority of the distribution. That is, the correction coefficient is made to be negative to reduce the overestimation. However, for the very extreme cases represented by AMDS that are actually not overestimated in the RAW, the negative correction coefficients, on the contrary, distort the distribution of extremes.

9

377 In all, the above analyses show the benefits and necessity of BC for post-processing either GCM or RCM
378 output before applying them to the HMs. It is useful in improving the simulated streamflow especially when
379 there is a large bias in the original climate simulations. However, the BC may cause the problem in the very
380 extreme values (e.g., AMDS) when the signal of their bias is different from that in the majority of the
381 distribution.

3.3 Reducing the uncertainty in future streamflow projection

383 For the streamflow projection for the future, Fig. 10 presents the spatial pattern of the relative change in the
384 runoff during wet season from the hydrological simulations driven by RAW climate simulations and the
385 ensemble mean of the hydrological simulations driven by same CM data corrected by four different BC
386 methods (i.e., ENSBC). The signal of the intensified streamflow occupies a large area in the target basins,
387 but disagreement among the models can still be seen where uncertainty has been found in the projected
388 precipitation change, mainly in the middle of Korean Peninsula (Qiu and Im 2021). The simulated change of
389 streamflow follows a similar spatial pattern with precipitation for all the models in all the resolutions, which
390 is understandable because precipitation takes up the major contribution to wet season river runoffs. The inter-
391 model uncertainty is highly subject to the levels of warming in the corresponding GCMs, that the decreasing
392 signals appear over the middle and south part of the country under a low warming level (i.e., CCSM4 in this
393 study). Similar precipitation change pattern were projected in previous downscaling studies with other GCMs
394 and RCMs (Kim et al. 2018; Oh and Suh 2018), and such uncertainty in precipitation projection is then
395 reflected on the streamflow projection.

396 On the other hand, for the comparison between RAW and ENSBC, the simulated runoff from bias-corrected
397 meteorological conditions shows a qualitatively similar pattern with RAW in terms of the change signal and
398 spatial distribution. However, the coarse resolution shows quite a large difference in the projected change
399 magnitude with and without BC. For example, the relative change in NorESM$_{GCM\_ENSBC}$ is more than two
400 times that in NorESM$_{GCM\_RAW}$. Such a large difference in the hydrological simulations driven by climate
401 conditions with and without BC is a non-negligible uncertainty in the understanding of the projected change.

402 Compared to the seasonal mean, the high flows may need more of our attention due to their severe impacts
403 on human society. Thus, to have a deeper investigation of how the resolution of dynamical downscaling and
404 statistical BC affect the streamflow projections, Fig. 11 presents the relative change of two high flow indexes,
405 i.e., AMDS and Q95 (the daily streamflow exceeded 95% of the time throughout the year), from all the
406 hydrological simulations. Note that the high flow indexes in Fig. 11 are derived on a basin basis rather than
407 a grid basis. That is, the daily streamflow of each grid point is summed up over the basin first before
408 calculating the indexes. The black is from the RAW and different colors are for different BC methods. Similar
409 to the mean of wet season, the result shows that all the simulations project the high flow to increase. Also,
410 the high flow may likely witness a considerably larger magnitude of increase than the seasonal mean, which
411 is consistent with the general finding that the heavy precipitation will increase more intensely than the
412 average.

413 However, one thing that should be stressed is that the discrepancy in the projected change among the BC
414 methods varies with the climate simulation resolution. There is a distinctly smaller range of spread among
415 the different BC methods for WRF05-driven hydrological simulations than those driven with WRF20 and
416 GCM in the projected increase. For example, the NorESM$_{GCM}$ with different BC methods shows an increasing
417 rate from 60% to 110% for the AMDS over NRB, while that range for NorESM$_{WRF05}$ is less than 3%. The
418 large spread brought with different BC methods in the GCM-driven hydrological simulations can be
419 significantly reduced by the downscaling with increasing resolution, which can be seen as the reduction of
420 uncertainty in the projected result. Especially for WRF05, not only is the deviation range narrowed among
421 different BC methods, the projected high flow change driven by meteorological conditions with and without

422 BC is also relatively small. This result is very meaningful because if the difference brought with BC methods
423 can lead to such large uncertainty in the result, then it is hard to tell if the projected streamflow change is
424 reliable or not. Especially, hydrological projections normally just use one or two BC methods to correct the
425 meteorological variables. It is very likely that they simply rely on the bias-corrected result during the
426 historical period but ignore such huge uncertainty in the projected streamflow change.

427 **4. Discussion and summary**

428 This study investigates the effect of very-high-resolution dynamical downscaling in the application of
429 hydrological impact assessment. Although the benefits of RCM have been elaborated by comparing against
430 observation and exploring the physical mechanisms behind it in many previous studies, the direct evaluation
431 in hydrological implication may be more straightforward and meaningful for the end users (e.g., hydrological
432 modeling community). In this regard, we use the multi-model, multi-resolution climate simulation ensemble
433 to feed HM in combination with different BC methods to project the streamflow change in South Korea at
434 the end of the 21st century. Three CMIP5 GCMs are downscaled into WRF20 and WRF05, and four BC
435 methods covering simple-to-complicated approaches are used for post-processing the climate data to
436 facilitate a comprehensive assessment.

437 The results from the original climate simulations and the hydrological simulations driven by RAW show that
438 high-resolution dynamical downscaling can significantly improve the simulated meteorological and
439 hydrological variables, while we also acknowledge that BC plays an indispensable role in reducing the
440 systematic bias in CM. However, although the bias-corrected product seems similar for the simulated
441 seasonal mean during the REF period, this does not mean that BC would erase the added value of high-
442 resolution RCM. From the one side, WRF05 still preserves a better performance than GCM and WRF20 after
443 BC for the reproduction of spatial variability and extreme indices in the REF period. On the other hand, more
444 importantly, the higher resolution downscaling can help reduce the uncertainty of the projected change
445 brought by BC.

446 For all the hydrological simulations considered, they agree with an increase in wet season streamflow and
447 especially the high flows over the targeted basins for the future. However, discrepancies can be found among
448 the hydrological simulations driven by different GCMs, different resolutions of RCM, and the climate
449 simulation post-processed by different BC methods. Although the projected streamflow change generally
450 follows the pattern of change in the simulated precipitation, it is found that the improved representation in
451 WRF05 can help reduce the uncertainty brought by different BC methods in the projected streamflow change,
452 particularly for the high flows. The non-negligible bias in the coarse-resolution climate simulations during
453 the REF period, on the contrary, leads to the large correcting coefficients that are very likely to induce
454 considerable difference among different BC methods for the projected change, which greatly impairs the
455 reliability of the subsequent hydrological projections.

456 Currently, there are more and more high-resolution dynamically-downscaled climate products available, but
457 there is still a long way to go for advertising their value to the end-users. Thus, the added value assessment
458 of high resolution RCM should not be limited to region-specific climate features; a straightforward
459 comparison for the hydrological simulations driven by different CM products may enable a more convincing
460 evaluation from the perspective of impact assessment application. Note that this study does not neglect the
461 effect of the statistical post-processing tools. On the other hand, we emphasize that the high resolution
462 dynamical downscaling can reduce the uncertainty in BC while acknowledging the effect of BC on removing
463 the systematic bias in climate simulations. Some studies stick to using GCMs for driving HM because they
464 argue that BC is enough for reducing the bias seen in the reference period. However, this study points out
465 that although the bias-corrected product seems "excellent" during the reference period, there can be a
466 significant difference in the projected change using different BC methods. While previous study also pointed

11

467 out the impact of BC on runoff will increase with the bias of CMs (Muerth et al. 2013), this study is the first
468 trial from the perspective of the large ensemble projections to assess the impact the very-high-resolution in
469 dynamical downscaling to the modeling chain of CM-BC-HM. Although we do not explicitly quantify the
470 uncertainty contribution from each source, which is not the focus of this study, we clearly demonstrate that
471 the high-resolution RCM can narrow the spread from different BC methods and thus reduce the uncertainty
472 in the hydrological projections.

473 Altogether, the comparative assessment provides valuable information for understanding the hydrological
474 change under global warming of this region and for assessing the resolution effect in the model chain of
475 climatic – hydrological simulations. Especially, the added value found in the hydrological application is not
476 common, and it offers an added value in a wide-ranging context and thus can serve to advance the
477 understanding and utilization of climate downscaling. Also, although some of the projected changes are
478 consistent with the findings in previous studies, the generated hydroclimate dataset still provides an
479 unprecedented multi-model, high-resolution ensemble of hydrological projections for this region. It is
480 meaningful for the scientific and end-user communities for the process understanding and impact assessment.

481 For further study, more HMs should be considered for a better understanding of the uncertainty stemming
482 from the HM structure, allowing a more comprehensive assessment of the climate-hydrology model chain.
483 In particular, the HM applied, VIC, is a semi-distributed model. Therefore, it is necessary to evaluate and
484 compare the uncertainty from HMs with a different structure such as lumped models or fully-distributed
485 models. Also, only one resolution, 12.5 km, is applied for the HM. For thoroughly examining the effect of
486 high resolution dynamical downscaling, a larger ensemble of HM with different resolutions may help gain a
487 clearer idea of the appropriate resolution necessary for a reasonable hydrological climate change impact
488 assessment.

489 **Reference**
490 Ahn SR, Kim SJ (2016) Assessment of climate change impacts on the future hydrologic cycle of the Han
491   River Basin in South Korea using a grid-based distributed model. Irrig Drain 65:11-21.
492   https://doi.org/10.1002/ird.1963
493 Anjum MN, Ding Y, Shangguan D (2019) Simulation of the projected climate change impacts on the river
494   flow regimes under CMIP5 RCP scenarios in the westerlies dominated belt, northern Pakistan. Atmos
495   Res 227:233-248. https://doi.org/10.1016/j.atmosres.2019.05.017
496 Aryal A, Shrestha S, Babel MS (2019) Quantifying the sources of uncertainty in an ensemble of hydrological
497   climate-impact projections. Theor Appl Climatol 135:193-209. https://doi.org/10.1007/s00704-017-
498   2359-3
499 Bae D-H, Koike T, Awan JA, Lee M-H, Shon K-He (2015) Climate change impact assessment on water
500   resources and susceptible zones identification in the Asian Monsoon region. Water Resour Manag
501   29:5377-5393. https://doi.org/10.1007/s11269-015-1124-6
502 Bedia J, Baño-Medina J, Legasa MN, Iturbide M, Manzanas R, Herrera S, Casanueva A, San-Martin D,
503   Cofino AS, Gutierrez M (2020) Statistical downscaling with the "downscaleR" package (v3.1.0):
504   contribution to the VALUE intercomparison experiment. Geosci Model Dev 13:1711-1735.
505   https://doi.org/10.5194/gmd-13-1711-2020
506 Bosshard T, Carambia M, Goergen K, Kotlarski S, Krahe P, Zappa M, Schär C (2013) Quantifying uncertainty
507   sources in an ensemble of hydrological climate-impact projections. Water Resour Res 49:1523-1536.
508   https://doi.org/10.1029/2011WR011533
509 Cannon AJ (2018) Multivariate quantile mapping bias correction: an N-dimensional probability density
510   function transform for climate model simulations of multiple variables. Clim Dyn 50:31-49.
511   https://doi.org/10.1007/s00382-017-3580-6
512 Cannon AJ (2020) R Package 'MBC': Multivariate Bias Correction of Climate Model Outputs
513 Cannon AJ, Sobie SR, Murdock TQ (2015) Bias correction of GCM precipitation by Quantile Mapping: How
514   well do methods preserve changes in quantiles and extremes? J Clim 28:6938-6959.

515   https://doi.org/10.1175/JCLI-D-14-00754.1

516 Chen F, Dudhia J (2001) Coupling an advanced land surface – hydrology model with the Penn State – NCAR
517   MM5 Modeling System. Part I : Model implementation and sensitivity. Mon Weather Rev 129:569-
518   585. https://doi.org/10.1175/1520-0493(2001)129<0569:caalsh>2.0.co;2

519 Giorgi F, Gutowski WJ (2015) Regional dynamical downscaling and the CORDEX Initiative. Annu Rev
520   Environ Resour 40:467-490. https://doi.org/10.1146/annurev-environ-102014-021217

521 Haddeland I, Heinke J, Voß F, Eisner S, Chen C, Hagemann S, Ludwig F (2012) Effects of climate model
522   radiation, humidity and wind estimates on hydrological simulations. Hydrol Earth Syst Sci 16:305-318.
523   https://doi.org/10.5194/hess-16-305-2012

524 Haider H, Zaman M, Liu S, Saifullah M, Usman M, Chauhdary JN, Anjum MN, Waseem M (2020) Appraisal
525   of climate change and its impact on water resources of Pakistan: A case study of Mangla Watershed.
526   Atmosphere 11:1071. https://doi.org/10.3390/atmos11101071

527 Hamman JJ, Nijssen B, Bohn TJ, Gergel DR, Mao Y (2018) The Variable Infiltration Capacity model version
528   5 (VIC-5): infrastructure improvements for new applications and reproducibility. Geosci Model Dev
529   11:3481-3496. https://doi.org/10.5194/gmd-11-3481-2018

530 Held IM, Soden BJ (2006) Robust responses of the hydrological cycle to global warming. J Clim 19:5686-
531   5699. https://doi.org/10.1175/JCLI3990.1

532 Jacob D, Teichmann C, Sobolowski S, et al (2020) Regional climate downscaling over Europe: Perspectives
533   from the EURO-CORDEX community. Reg Environ Change 20:51. https://doi.org/10.1007/s10113-
534   020-01606-9

535 Jung IW, Bae DH, Lee BJ (2013) Possible change in Korean streamflow seasonality based on multi-model
536   climate projections. Hydrol Processes 27:1033–1045. https://doi.org/10.1002/hyp.9215

537 Kim G, Cha DH, Park C, et al (2018) Future changes in extreme precipitation indices over Korea. Int J
538   Climatol 38:e862-e874. https://doi.org/10.1002/joc.5414

539 Kim J-B, Im E-S, Bae D-H (2020) Intensified hydroclimatic regime in Korean basins under 1.5 and 2°C
540   global warming. Int J Climatol 40:1965-1978. https://doi.org/10.1002/joc.6311

541 Kotamarthi R, Hayhoe K, Mearns L, Wuebbles D, Jacobs J, Jurado J (2021) Added value of Downscaling.
542   In: Downscaling techniques for high-resolution climate projections: From global change to local
543   impacts. Cambridge University Press, Cambridge, pp102-120

544 Kundzewicz ZW, Kanae S, Seneviratne SI, et al (2014) Flood risk and climate change: global and regional
545   perspectives. Hydrol Sci J 59:1-28. https://doi.org/10.1080/02626667.2013.857411

546 Leander R, Buishand TA (2007) Resampling of regional climate model output for the simulation of extreme
547   river flows. J Hydrol 332:487-496. https://doi.org/10.1016/j.jhydrol.2006.08.006

548 Lee J-H, Park S-Y, Kim J-S, Sur C, Chen J (2018a) Extreme drought hotspot analysis for adaptation to a
549   changing climate: Assessment of applicability to the five major river basins of the Korean Peninsula.
550   Int J Climatol 38:4025-4032. https://doi.org/10.1002/joc.5532

551 Lee M-H, Bae D-H, Im E-S (2019a) Effect of the horizontal resolution of climate simulations on the
552   hydrological representation of extreme low and high flows. Water Resour Manag 33:4653–4666.
553   https://doi.org/10.1007/s11269-019-02359-9

554 Lee M-H, Lu M, Im E-S, Bae D-H (2018b) Added value of dynamical downscaling for hydrological
555   projections in the Chungju Basin, Korea. Int J Climatol 39:516-531. https://doi.org/10.1002/joc.5825

556 Lee M-H, Qiu L, Ha S, Im E-S, Bae D-H (2021) Future projection of low flows in the Chungju basin, Korea
557   and their uncertainty decomposition. Int J Climatol 1-18. https://doi.org/10.1002/joc.7237

558 Lee M-H, Im E-S, Bae D-H (2019b) A comparative assessment of climate change impacts on drought over
559   Korea based on multiple climate projections and multiple drought indices. Clim Dyn 53:389-404.
560   https://doi.org/10.1007/s00382-018-4588-2

561 Liang X, Lettenmaier DP, Wood EF, Burges SJ (1994) A Simple hydrologically based model of land surface
562   water and energy fluxes for general circulation models. J Geophys Res 99:14415-14428.
563   https://doi.org/10.1029/94JD00483

564 Maraun D (2016) Bias correcting climate change simulations - a critical review. Curr Clim Change Rep
565   2:211-220. https://doi.org/10.1007/s40641-016-0050-x

566 Maraun D, Shepherd TG, Widmann M, et al (2017) Towards process-informed bias correction of climate
567   change simulations. Nat Clim Change 7:764-773. https://doi.org/10.1038/nclimate3418

568 Maraun D, Wetterhall F, Chandler RE, et al (2010) Precipitation downscaling under climate change: Recent

569   developments to bridge the gap between dynamical models and the end user. Rev Geophys 48:RG3003.
570   https://doi.org/10.1029/2009RG000314

571 Muerth MJ, Gauvin St-Denis B, Ricard S, Velázquez JA, Schmid J, Minville M, Caya D, Chaumont D,
572   Ludwig R, Turcotte R (2013) On the need for bias correction in regional climate scenarios to assess
573   climate change impacts on river runoff. Hydrol Earth Syst Sci 17:1189-1204.
574   https://doi.org/10.5194/hess-17-1189-2013

575 Oh SG, Suh MS (2018) Changes in seasonal and diurnal precipitation types during summer over South Korea
576   in the late twenty-first century (2081-2100) projected by the RegCM4.0 based on four RCP scenarios.
577   Clim Dyn 51:3041-3060. https://doi.org/10.1007/s00382-017-4063-5

578 Qiu L, Im E-S, Hur J, Shim K-M (2020) Added value of very high resolution climate simulations over South
579   Korea using WRF modeling system. Clim Dyn 54:173-189. https://doi.org/10.1007/s00382-019-
580   04992-x

581 Ryu JH, Lee JH, Jeong S, Park SK, Han K (2011) The impacts of climate change on local hydrology and low
582   flow frequency in the Geum River Basin, Korea. Hydrol Processes 25:3437-3447.
583   https://doi.org/10.1002/hyp.8072

584 Safeeq M, Mauger GS, Grant GE, Arismendi I, Hamlet AF, Lee S-Y (2014) Comparing large-scale
585   hydrological model predictions with observed streamflow in the Pacific Northwest: Effects of climate
586   and groundwater. J Hydrometeorol 15:2501-2521. https://doi.org/10.1175/JHM-D-13-0198.1

587 Seo K-H, Ok J, Son J-H, Cha D-H (2013) Assessing future changes in the East Asian Summer Monsoon
588   using CMIP5 coupled models. J Clim 26:7662-7675. https://doi.org/10.1175/JCLI-D-12-00694.1

589 Seo SB, Kim Y-O, Kim Y, Eum H-I (2019) Selecting climate change scenarios for regional hydrologic impact
590   studies based on climate extremes indices. Clim Dyn 52:1595-1611. https://doi.org/10.1007/s00382-
591   018-4210-7

592 Seo SB, Sinha T, Mahinthakumar G, Sankarasubramanian A, Kumar M (2016) Identification of dominant
593   source of errors in developing streamflow and groundwater projections under near-term climate change.
594   J Geophy Res Atmos 121:7652-7672. https://doi.org/10.1002/2016JD025138

595 Skamarock WC, Klemp JB, Dudhia J, et al (2021) A description of the Advanced Research WRF Model
596   Version 4.3. https://doi.org/10.5065/1dfh-6p97

597 Stefanidis K, Panagopoulos Y, Mimikou M (2018) Response of a multi-stressed Mediterranean river to future
598   climate and socio-economic scenarios. Sci Total Environ 627:756-769.
599   https://doi.org/10.1016/j.scitotenv.2018.01.282

600 Sun W, Wang Y, Wang G, Cui X, Yu J, Zuo D, Xu Z (2017) Physically based distributed hydrological model
601   calibration based on a short period of streamflow data: Case studies in four Chinese basins. Hydrol
602   Earth Syst Sci 21:251-265. https://doi.org/10.5194/hess-21-251-2017

603 Taylor KE, Stouffer RJ, Meehl GA (2012) An overview of CMIP5 and the experiment design. Bull Am
604   Meteorol Soc 93:485-498. https://doi.org/10.1175/BAMS-D-11-00094.1

605 Teutschbein C, Seibert J (2012) Bias correction of regional climate model simulations for hydrological
606   climate-change impact studies: Review and evaluation of different methods. J Hydrol 456-457:12-29.
607   https://doi.org/10.1016/j.jhydrol.2012.05.052

608 Vetter T, Huang S, Aich V, Yang T, Wang X, Krysanova V, Hattermann F (2015) Multi-model climate impact
609   assessment and intercomparison for three large-scale river basins on three continents. Earth Syst Dyn
610   6:17-43. https://doi.org/10.5194/esd-6-17-2015

611 Vetter T, Reinhardt J, Flörke M, et al (2017) Evaluation of sources of uncertainty in projected hydrological
612   changes under climate change in 12 large-scale river basins. Clim Change 141:419-433.
613   https://doi.org/10.1007/s10584-016-1794-y

614 Zaman M, Naveed Anjum M, Usman M, Ahmad I, Saifullah M, Yuan S, Liu S (2018) Enumerating the effects
615   of climate change on water resources using GCM scenarios at the Xin'anjiang Watershed, China. Water
616   10: 1296. https://doi.org/10.3390/w10101296

617 Zhang L, Yuan F, Wang B, et al (2021) Quantifying uncertainty sources in extreme flow projections for three
618   watersheds with different climate features in China. Atmos Res 249:105331.
619   https://doi.org/10.1016/j.atmosres.2020.105331

620   Zhang X, Alexander L, Hegerl GC, Jones P, Tank AK, Peterson TC, Trewin B, Zsiers FW (2011) Indices
621   for monitoring changes in extremes based on daily temperature and precipitation data. WIREs
622   Clim Change 2:851-870. https://doi.org/https://doi.org/10.1002/wcc.147
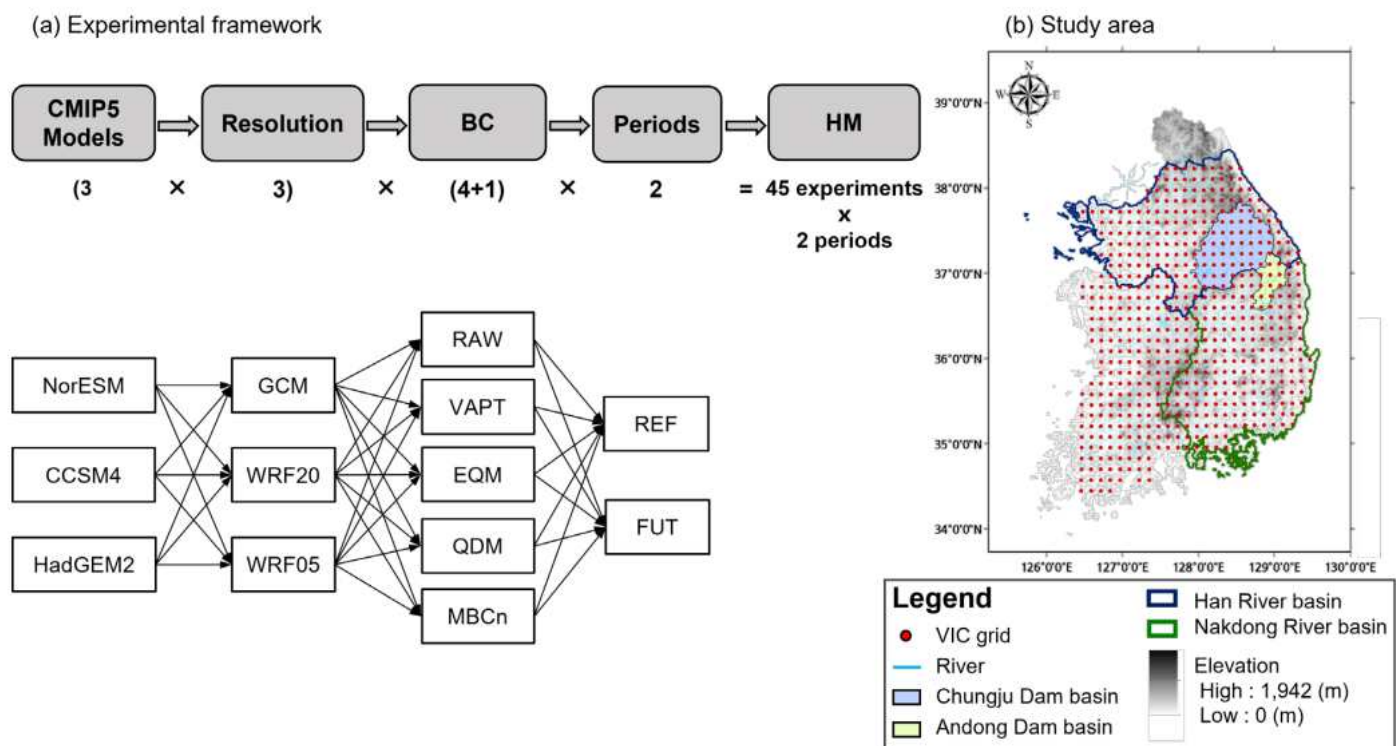
Figures

Figure 1

(a) Experimental framework that shows the combinations of different CMIP5 models, CM resolutions, and BC methods; (b) Elevation map of the study area derived from the 30-m Digital Elevation Map (unit: m) and the grid system employed by the VIC model in 0.125° grid over South Korea. The tributaries of the main rivers are marked by the light blue lines. This study focuses on Han River basin (HRB) and Nakdong River basin (NRB) outlined by the thick blue and green lines, respectively. The Chungju and Andong dam basins (shaded area) are selected for validation for HRB and NRB respectively.
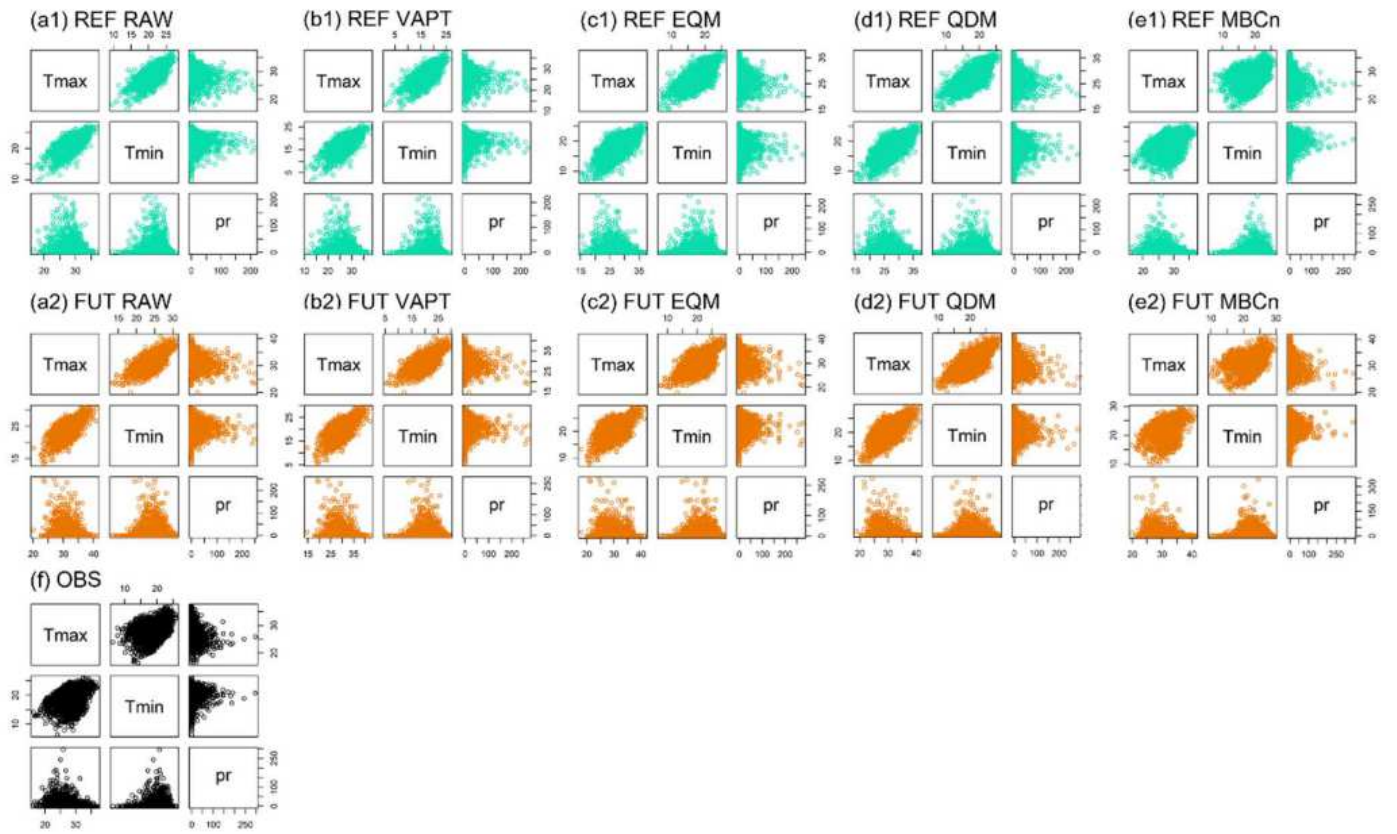
Figure 2

Illustrative example of the correlation matrices among daily Tmax, Tmin, and precipitation (pr) during JJAS from (a) OBS, (b) RAW, and (c-f) BC products using VAPT, EQM, QDM and MBCn for (1) REF and (2) FUT for a randomly select grid in CCSM4WRF05-REF.
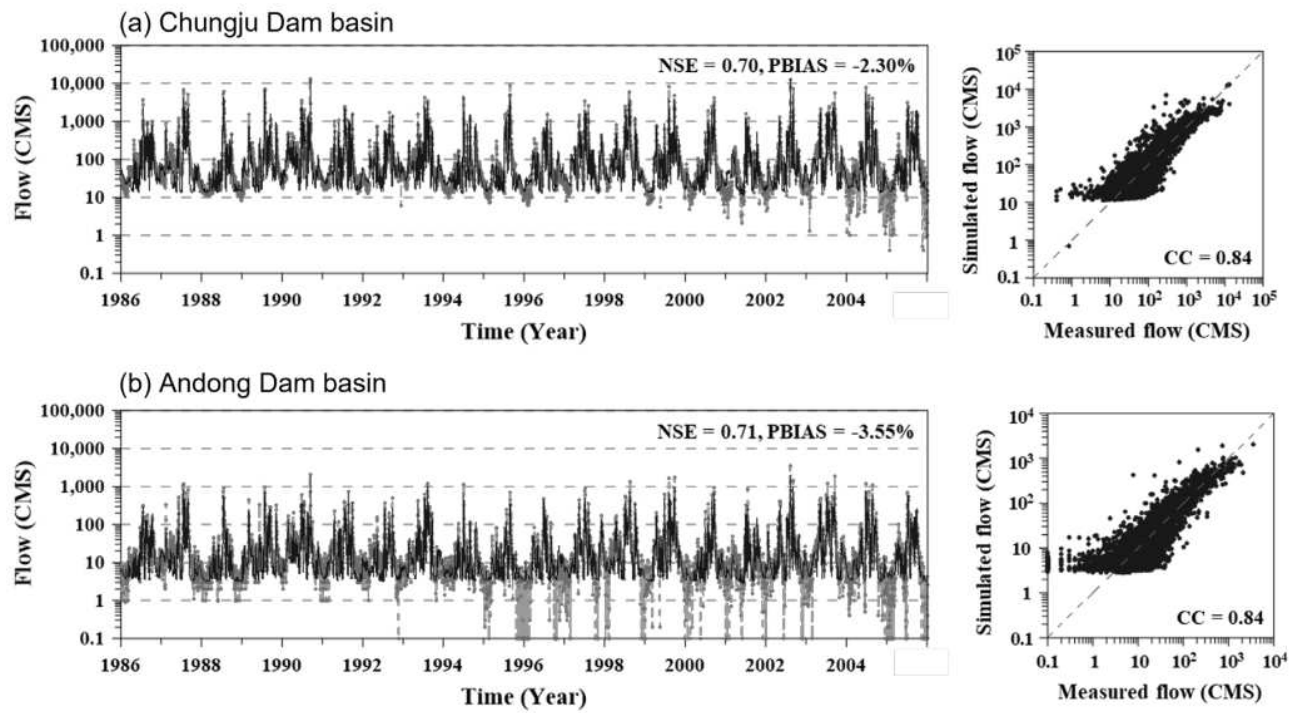
Figure 3

(left column) The daily time series of measured inflow and simulated streamflow in observational run; and (right column) the scatter plot of daily measured inflow (x-axis) versus observational run simulated streamflow (on the y-axis) in the (a) Chungju dam basin and (b) Andong dam basin (unit: CMS).
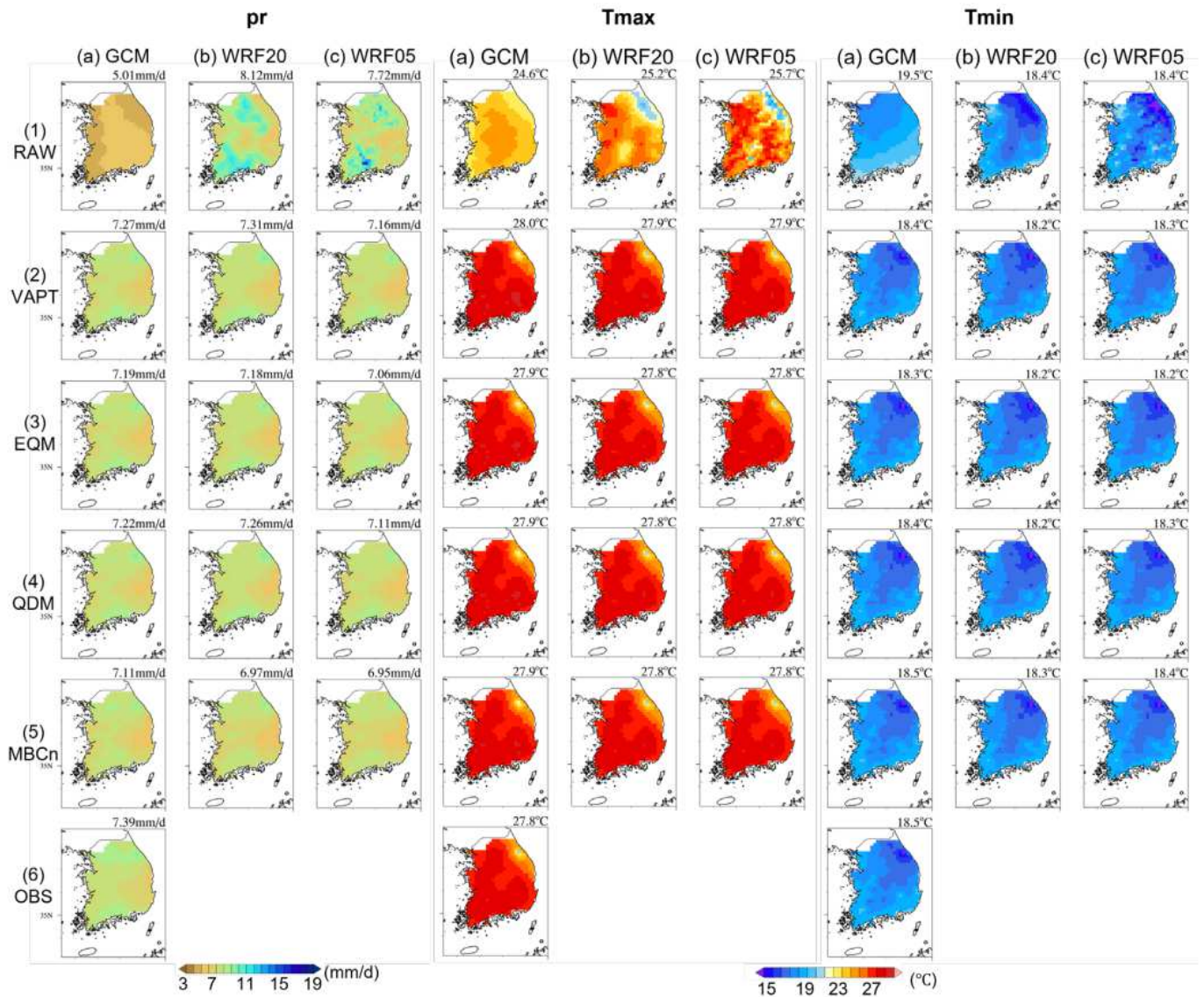
Figure 4

Spatial maps of climatological mean precipitation (pr), Tmax, and Tmin in JJAS from (a) ENSGCM-REF, (b) ENSWRF20-REF, and (c) ENSWRF05-REF of (1) RAW and its BC products using (2) VAPT, (3) EQM, (4) QDM, and (5) MBCn. (6) is the OBS used as the reference for BC. The value at the top right of each sub-figure is the spatial-average value over South Korea land.

Figure 5

Plot showing the proportion of grid points passing local K-S diagnostic tests for each ETTCDI index (row 1-6) and JJAS mean precipitation (pr), Tmax, and Tmin (row 7-9) during REF for (a) GCM; (b) WRF20; and (c) WRF05. The letter "C" stands for result from "CCSM4", "N" for "NorESM", "H" for "HadGEM2".

Figure 6

Spatial maps of the relative change (FUT vs. REF, unit: %) of climatological mean pr, Tmax, and Tmin in JJAS from (a) ENSGCM, (b) ENSWRF20, and (c) ENSWRF05 of (1) RAW and its BC products using (2)

VAPT, (3) EQM, (4) QDM, and (5) MBCn. The value at the top right of each sub-figure is the spatial-average value over South Korea land.
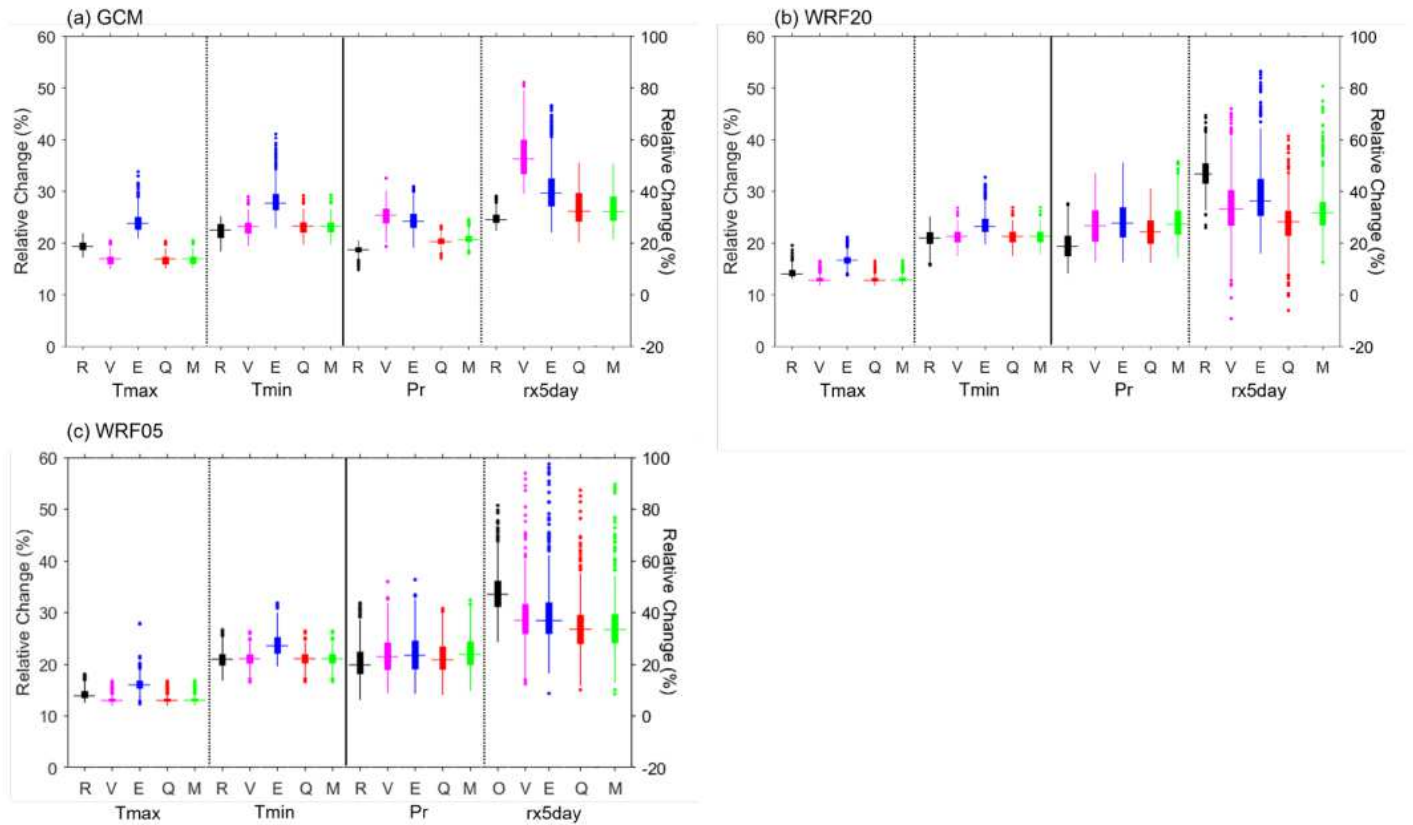
Figure 7

Boxplots of the relative change (FUT vs. REF, unit: %) in wet season mean Tmax & mean Tmin (left y-axis), and wet season mean Pr and rx5day (right y-axis) at each grid cell over the South Korea domain (land only) from (a) ENSGCM, (b) ENSWRF20, and (c) ENSWRF05. "R", "V", "E", "Q", and "M" stand for RAW, VAPT, EQM, QDM and MBCn respectively. The median change over the domain is given by the central line within each box.
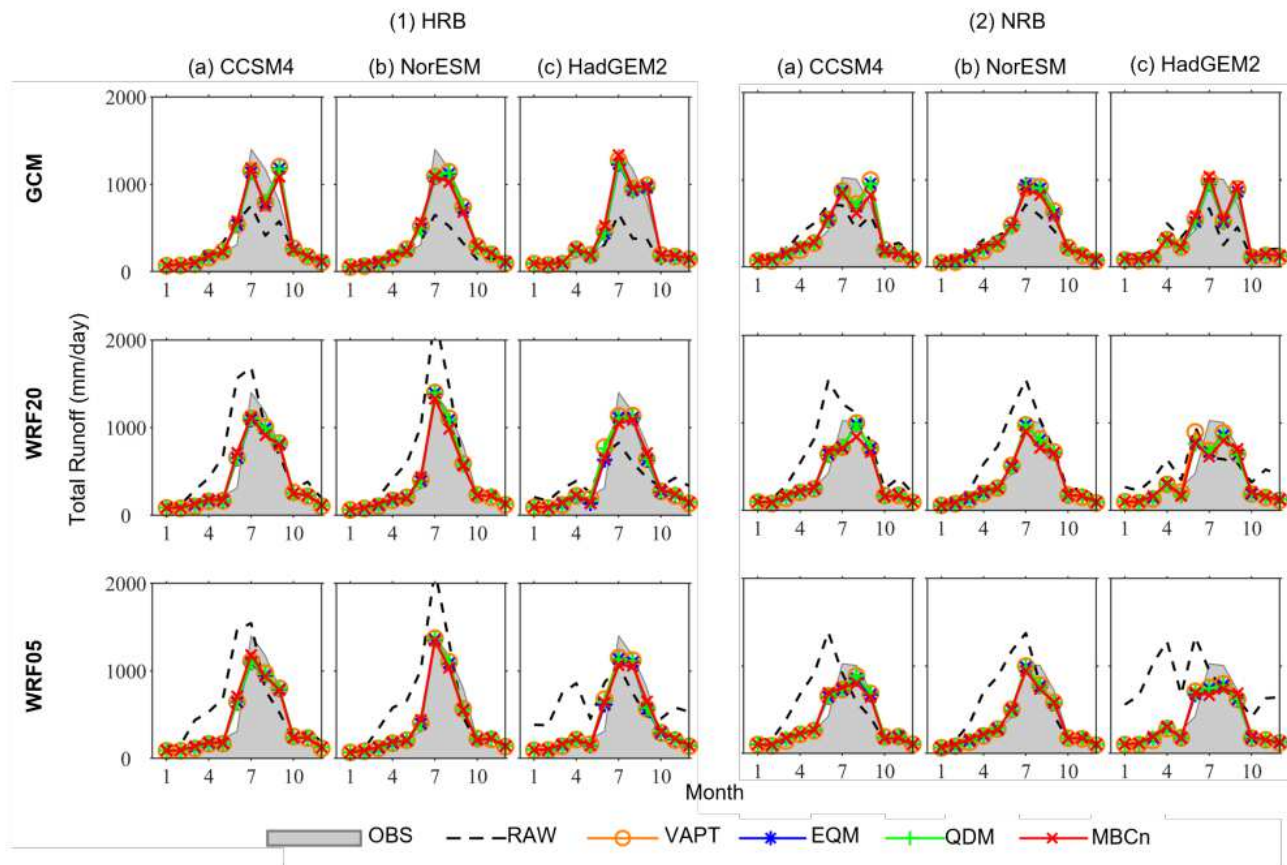
Figure 8

Annual cycle of the climatological monthly mean total runoff during REF over (1) HRB and (2) NRB. The lines are from hydrological simulations driven by (a) CCSM4, (b) NorESM, and (c) HadGEM2 in GCM (first row), WRF20 (second row), and WRF05 (third row). The shading is obtained from the hydrological simulation driven by OBS. The total runoff is obtained by adding all the streamflow values of HM grids within the basin.
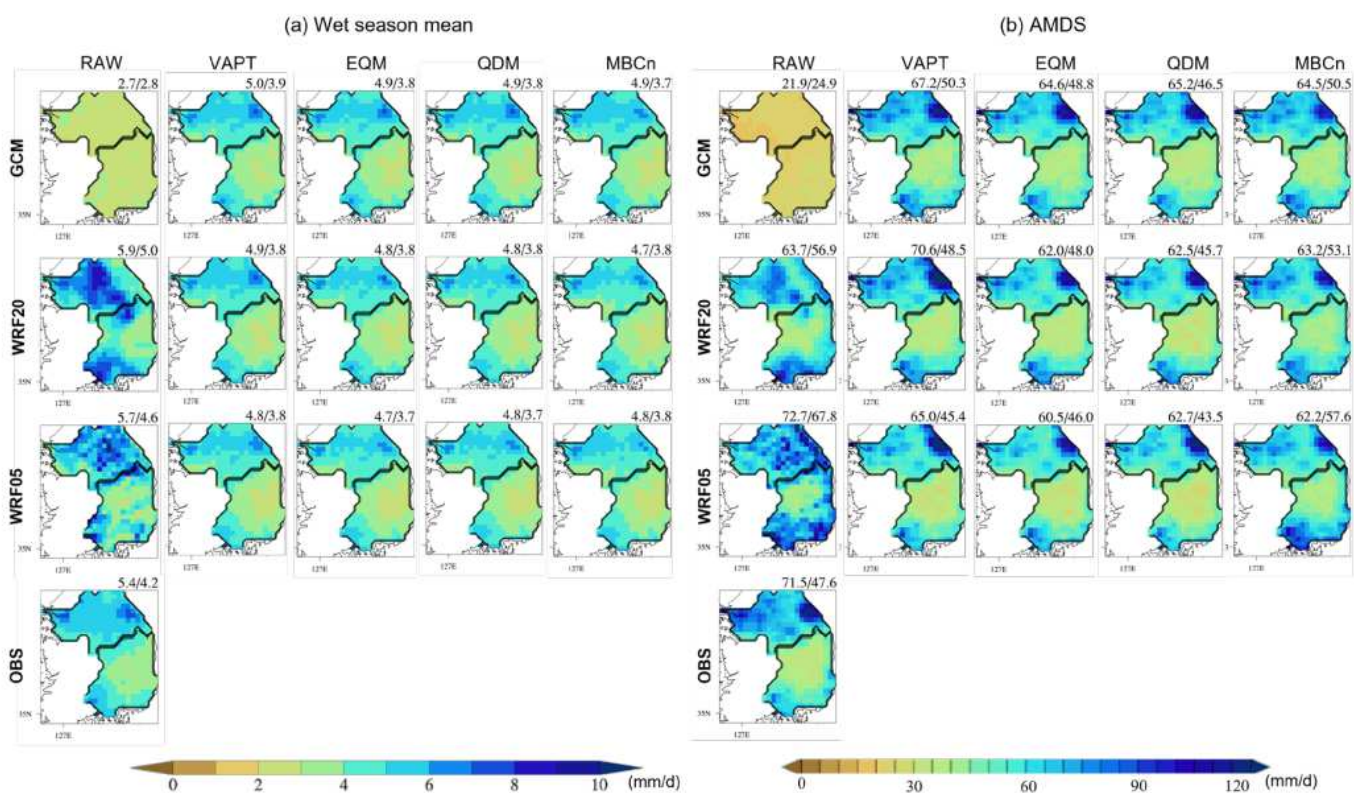
Figure 9

Spatial pattern over HRB and NRB of the 30-year mean runoff of (a) wet season mean (JJAS) and (b) the high flow represented by the Annual Maximum daily streamflow (AMDS) in ENSGCM (first row), ENSWRF20 (second row), and ENSWRF05 (third row) for hydrological projections using different BC methods and RAW. The fourth row is from OBS run. The value on the top-right corner is the spatial-average runoff over HRB/NRB. The unit is mm/day.
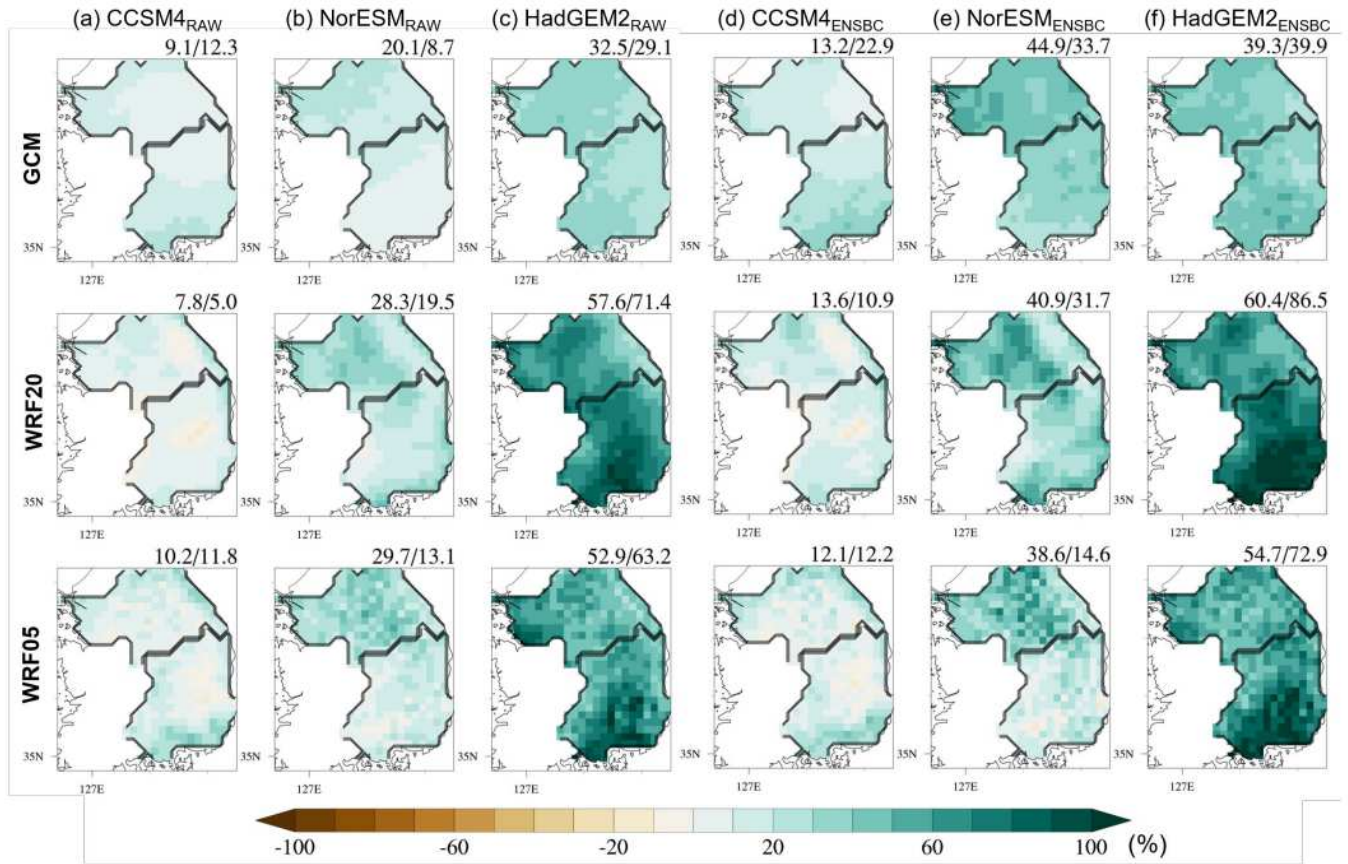
Figure 10

Spatial pattern of the relative change (%, FUT vs. REF) of simulated runoff during wet season over HRB and NRB from (a,e) CCSM, (b,f) NorESM, (c,g) HadGEM2. (a-d) is from RAW and (e-h) the ensemble mean of those corrected by VAPT, EQM, QDM, and MBCn. The value on the top-right corner is the spatial-average runoff over HRB/NRB.
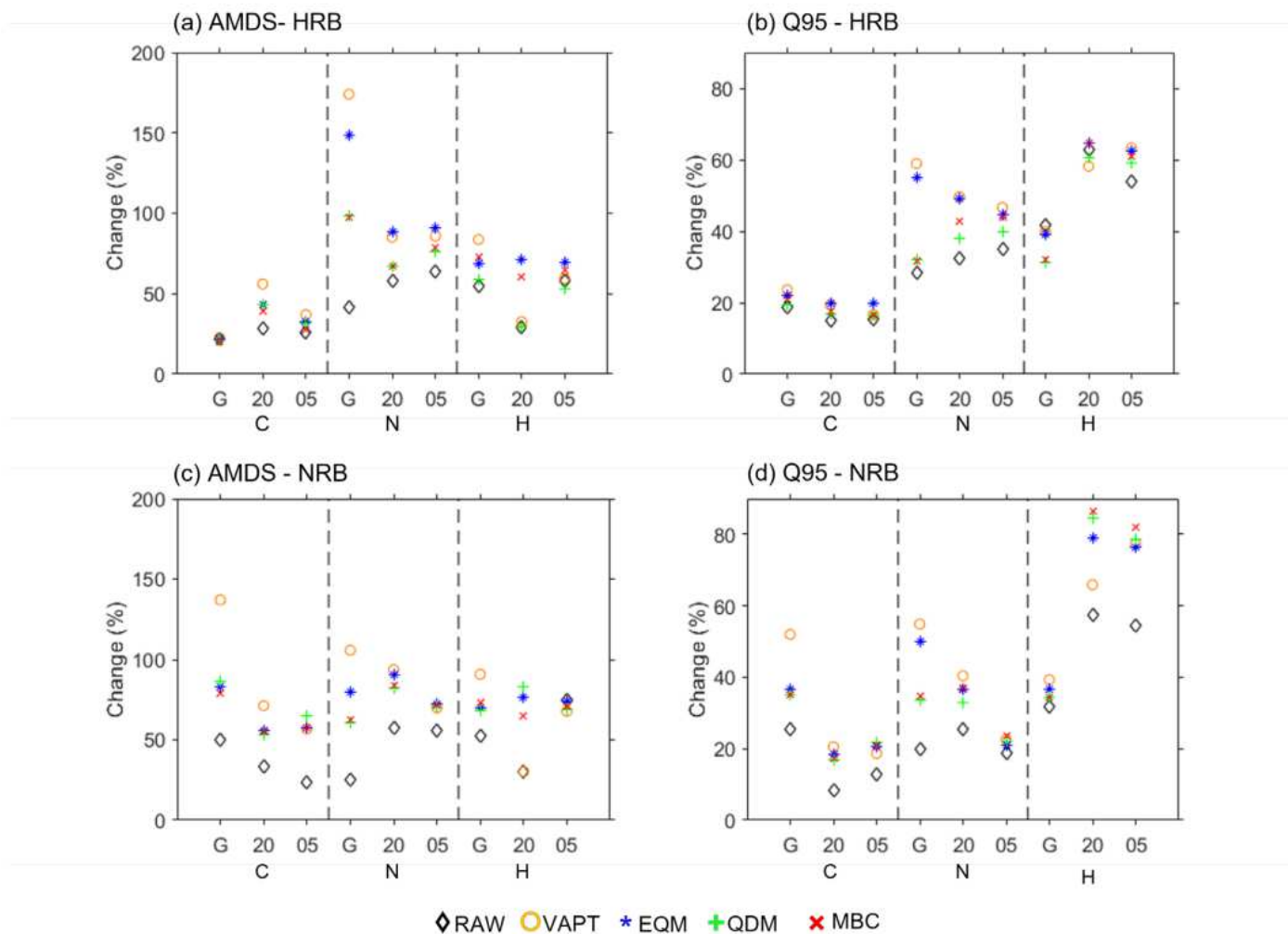
Figure 11

Relative change (FUT vs. REF, unit: %) of high flow indexes of (a,c) AMDS and (b,d) Q95 over the (a-b) HRB and (c-d) NRB from different hydrological simulations. "C", "N", "H" stand for CMIP5 models of "CCSM4", "NorESM" and "HadGEM2", and "G", "20", "05" stand for the resolution of "GCM", "WRF20", and "WRF05".